

Structures and electronic states of Mg incorporated into InN surfaces

Toru Akiyama, Kohji Nakamura, and Tomonori Ito
*Department of Physics Engineering, Mie University,
1577 Kurima-Machiya, Tsu 514-8507, Japan*

Jung-Hwan Song and Arthur J. Freeman
*Department of Physics and Astronomy,
Northwestern University, Evanston, Illinois 60208, USA*

(Dated: July 21, 2009)

Abstract

Structures and electronic states of Mg-incorporated into InN surfaces in various orientations including nonpolar $(10\bar{1}0)$ and $(11\bar{2}0)$ as well as polar (0001) and $(000\bar{1})$ surfaces are systematically investigated by performing first-principles pseudopotential calculations. Employing a thermodynamic approach, the calculated surface energies demonstrate characteristic features in the stability of Mg-incorporated surfaces depending on the growth condition. The calculated density of states also predict that regardless of surface orientation, Mg acceptors at the surface are compensated by the extra electrons originating from the surface states of In layers in bare surfaces.

PACS numbers: 68.43.Fg, 68.55.Ln, 73.20.Hb, 73.61.Ey

Ever since the discovery of its narrow energy gap,^{1,2} much attention has been attracted to InN for applications such as high-efficiency solar cells, light-emitting diodes, and high-frequency transistors. To realize these devices, the ability to fabricate both *p*-type and *n*-type InN through doping remains a key challenge. Especially, *p*-type doping in InN has been very difficult to achieve due to its propensity for *n*-type carrier formation.

Recently, buried *p*-type conductivity has been confirmed on In-polar samples which are grown along [0001] orientation, indicating the realization of *p*-type InN by Mg doping.³⁻⁶ Furthermore, the reduction of electron concentration in the electron accumulation layer of the surface was observed by Hall measurements, indicating carrier compensation due to *p*-type doping.^{5,6} Since these experimental results reveal donor-acceptor interactions on polar InN surfaces, they raise interesting issues such as the stability of Mg at the surface and its interaction with the electron accumulation layer. Although the stabilization of donors and acceptors on InN(000 $\bar{1}$) surface by the compensation mechanism has been envisioned using the highly precise full-potential linearized augmented plane-wave method,⁷ the formation of Mg-incorporated surfaces considering the growth condition and its effects on the electronic properties still remain unresolved problems.

Another important issue in InN is the growth and *p*-type doping along nonpolar orientation such as (10 $\bar{1}$ 0) and (11 $\bar{2}$ 0): These nonpolar planes are attractive because of the absence of polarization fields,^{8,9} whereas the growth of InN epitaxial films along polar orientations such as [0001] and [000 $\bar{1}$] may result in large polarization fields along the growth direction reducing the radiative efficiency.¹⁰ So far, x-ray photoemission spectroscopy (XPS)¹¹ and scanning photoelectron microscopy and spectroscopy¹² have observed electron accumulation on (10 $\bar{1}$ 0) planes, and calculations for the reconstructions on nonpolar InN(10 $\bar{1}$ 0) and (11 $\bar{2}$ 0) surfaces have clarified that the surfaces with In adlayers are favorable under In-rich conditions.^{13,14} These experimental and theoretical studies inspired us to predict the stability of Mg-incorporated surfaces taking account the growth (doping) conditions and the compensation mechanism due to Mg-doping in nonpolar orientations.

In this paper, we report extensive first-principles pseudopotential calculations to clarify effects of Mg atoms on the structure and electronic states for a variety of orientations including polar (10 $\bar{1}$ 0) and (11 $\bar{2}$ 0) as well as nonpolar (0001) and (000 $\bar{1}$). The calculated surface formation energies taking account of growth conditions reveal that atomic arrangements depending on surface orientation play an important role in Mg incorporation: InN(11 $\bar{2}$ 0)

surfaces are expected to be most preferable for Mg-incorporation. Our analysis of density of states also elucidates the compensation of Mg acceptors by accumulated electrons which originate from the surface states of In layers, as proposed in a previous study.⁷

The calculations are performed within density-functional theory using the generalized gradient approximation¹⁵ and ultrasoft pseudopotentials.^{16,17} Partial core corrections are used for 4*d* electrons of In atoms.¹⁸ The surface electronic states are analyzed using modified pseudopotentials. Atom centered repulsive potentials of Gaussian shape^{14,19} are included in each of the pseudopotentials, to yield a direct band gap of 0.7 eV in bulk InN. The conjugate-gradient technique is utilized both for the electronic structure calculations and for geometry optimization.²⁰ The valence wave functions are expanded by the plane-wave basis set with a cutoff energy of 28 Ry. The surfaces are simulated using super slab models of five bilayers for (0001) and (000 $\bar{1}$) surfaces, and those of eight atomic layers for (10 $\bar{1}$ 0) and (11 $\bar{2}$ 0) surfaces, with ~ 12 Å vacuum region. The bottom surface of the slab is passivated with artificial hydrogen atoms and the lower four layers are fixed at ideal positions. We use a 36-*k* points sampling for the 1×1 surface unit, which provides sufficient accuracy in the total energy.

Assuming the surface in equilibrium with bulk InN, the relative stability among various Mg-incorporated surfaces is assessed using the formation energy E_f given by

$$E_f = E_{tot} - E_{ideal} - n_{\text{Mg}}\mu_{\text{Mg}} - (n_{\text{In}} - n_{\text{N}})\mu_{\text{In}} - n_{\text{N}}\mu_{\text{InN}}^{\text{bulk}}, \quad (1)$$

where E_{tot} and E_{ideal} are the total energy of the surface under consideration and of the reference (ideal) surface, respectively, μ_i is the chemical potential of the *i*th species, $\mu_{\text{InN}}^{\text{bulk}}$ is the chemical potential of bulk InN, and n_i is the number of excess or deficit *i*th atoms with respect to the reference. μ_{In} can vary in the thermodynamically allowed range $\mu_{\text{In}}^{\text{bulk}} + \Delta H_f \leq \mu_{\text{In}} \leq \mu_{\text{In}}^{\text{bulk}}$, where ΔH_f is the heat of formation of bulk InN ($\mu_{\text{In}}^{\text{bulk}}$ is the chemical potential of bulk In). The lower and upper limits correspond to N-rich and In-rich conditions, respectively. The calculated value of ΔH_f is -0.37 eV, which agrees with previous calculations^{13,21} and experiments.²² For the chemical potential of Mg, the temperature and pressure dependence of reservoirs is taken into account using $\mu_{\text{Mg}} = E_{\text{Mg}} + k_B T \ln(pV_Q/k_B T)$, where E_{Mg} is the total energy of isolated Mg atom, k_B is the Boltzmann constant, T is the temperature, and p is the pressure, and $V_Q = (h^2/2\pi m k_B T)^{3/2}$ is the quantum volume:^{23,24} The contribution of the second term varies from -3.0 to -2.5 eV depending on the pressure ($10^{-12} \leq p \leq 10^{-7}$ Torr) at $T=725$ K (typical molecular-beam epitaxy (MBE) growth conditions).

Polar planes. — Figure 1 shows the calculated formation energies of Mg-incorporated surfaces on (0001) and (000 $\bar{1}$) planes ($T=725$ and 825 K in μ_{Mg} , respectively) as a function of μ_{In} using the slab models with 2×2 and $\sqrt{3}\times\sqrt{3}$ periodicity along with those for bare surfaces.²⁵ In the absence of Mg, the surface with an In adatom (In_{ad}) on the T4 site and a laterally contracted In bilayer ($\text{In}_{\text{bilayer}}$) are stabilized for moderately and extreme In-rich conditions on the (0001) surface, respectively, while the surface with an In adlayer ($\text{In}_{\text{adlayer}}$) is favorable over the entire μ_{In} range on the (000 $\bar{1}$) surface.^{13,21} In addition to these reconstructions, we find that the reconstructions with In bilayer and In trilayer structures proposed by the XPS²⁶ for InN(0001) and (000 $\bar{1}$) surfaces, respectively, are stabilized only for extremely In-rich conditions satisfying $\mu_{\text{In}} \geq 0.1$ eV.

As shown in Fig. 1(a), in the presence of Mg on the InN(0001) surface, the 2×2 surface with three substitutional Mg atoms at the topmost In sites, $\text{Mg}_{\text{In}}(3/4)$, is found to be favorable over a wide range of μ_{In} among various surface reconstructions including bare surfaces. Besides, for low p in μ_{Mg} ($\sim 10^{-12}$ Torr), the surface with two substitutional Mg atoms, $\text{Mg}_{\text{In}}(1/2)$, is found to be stabilized (not shown here). This implies that Mg atoms can be easily incorporated on the surface and the fraction of substitutional Mg atoms at the topmost In sites increases with higher p , qualitatively consistent with the high Mg concentration obtained from secondary-ion-mass spectroscopy.⁶ The atomic configuration of $\text{Mg}_{\text{In}}(3/4)$ is identical to the most stable one in Mg-incorporated GaN(0001) surfaces,^{27,28} indicating that its stabilization can be interpreted in terms of the electron counting rule.²⁹ From total energy differences among various structures, we estimate that the energy deficit due to excess electrons on In dangling bonds³¹ and the bond-energy difference between In-N and Mg-N are ~ 0.65 eV/electron and ~ -0.1 eV (In-N bonds are stable), respectively. These values clearly show that excess electrons on In dangling bonds crucially affect the structural stability of (0001) surface.

Situations on the (000 $\bar{1}$) surface are different from those on the (0001) surface. The 2×2 surface with a substitutional Mg atom at the topmost In layer of $\text{In}_{\text{adlayer}} + \text{Mg}_{\text{In}}$ is the most stable among Mg-incorporated surfaces over the entire μ_{In} range, consistent with x-ray absorption fine structure measurements.³⁰ However, its formation energy is higher than that of $\text{In}_{\text{adlayer}}$, especially for In-rich conditions, as shown in Fig. 1(b). Since the formation energy difference between $\text{In}_{\text{adlayer}}$ and $\text{In}_{\text{adlayer}} + \text{Mg}_{\text{In}}$ is small under N-rich conditions, this indicates that the Mg-incorporated (000 $\bar{1}$) surfaces are always metastable under In-rich

conditions and appear occasionally under N-rich conditions.³² The stability of the $\text{In}_{\text{adlayer}}$ can be qualitatively understood by the preference of metallic In-In bonds compared to In-Mg bonds in the adlayer.

Figure 2 shows the calculated density of states (DOS) of Mg-incorporated surfaces, along with those of bare surfaces. The absence of electronic states around the Fermi energy is found in the DOS of $\text{Mg}_{\text{In}}(3/4)$ (solid line in Fig. 2(a)), exhibiting semiconducting character satisfying the electron counting rule.²⁹ Comparison with the DOS of $\text{In}_{\text{bilayer}}$ (dashed line in Fig. 2(a)) also clarifies that the electronic states, which could be responsible for the electron accumulation, are reduced by Mg-incorporation, leading to the reduction of electron concentration reported in the experiments^{3,4,6} In contrast, around the Fermi energy the DOS of $\text{In}_{\text{adlayer}}+\text{Mg}_{\text{In}}$ is similar to that of $\text{In}_{\text{adlayer}}$, as shown in Fig. 2(b). This is because the states near the Fermi energy correspond to metallic In-In bonds in the In adlayer and there are little changes even after substitution by one Mg atom. We note that the local DOS for N atoms near Mg at the surface for $\text{Mg}_{\text{In}}(3/4)$ and for $\text{In}_{\text{adlayer}}+\text{Mg}_{\text{In}}$ shown in Figs. 2(a) and 2(b), respectively, are virtually occupied by electrons: Mg acceptors at the surface are neutralized/compensated by electrons from the surfaces, supporting the experimental data.^{3,4,6}

Nonpolar planes. — Since both In and N atoms appear on ideal nonpolar planes, Mg-incorporated structures on $\text{InN}(10\bar{1}0)$ and $(11\bar{2}0)$ surfaces inherit the structural characteristics of both polar (0001) and $(000\bar{1})$ planes together. Figure 3 shows the calculated formation energies of $\text{InN}(10\bar{1}0)$ and $(11\bar{2}0)$ planes as a function of μ_{In} (at $p=1.0\times 10^{-7}$ Torr and $T=725$ K in μ_{Mg}) using slab models with 1×2 and 1×1 periodicity for $(10\bar{1}0)$ and $(11\bar{2}0)$, respectively.²⁵ In the absence of Mg, the surfaces with a laterally contracted In bilayer ($\text{In}_{\text{bilayer}}$) and with an In adlayer ($\text{In}_{\text{adlayer}}$) shown in Figs. 4(a) and 4(c) are favorable for the $(10\bar{1}0)$ and $(11\bar{2}0)$ surfaces, respectively. For $\text{InN}(11\bar{2}0)$ surface, the calculated formation energy of $\text{In}_{\text{bilayer}}$ is higher than that of $\text{In}_{\text{adlayer}}$. Since the surface area per topmost atom on $(11\bar{2}0)$ surface is small, the distances between In adatoms in $\text{In}_{\text{bilayer}}$ on the $(11\bar{2}0)$ surface ($\sim 3.02\text{\AA}$) become smaller than the In-In bond length (3.28\AA) in bulk In. The energy profit by forming $\text{In}_{\text{bilayer}}$ on the $(11\bar{2}0)$ surface seems to be smaller than that on the $(10\bar{1}0)$ surface due to stronger Coulomb repulsion.

Unlike the results for $\text{GaN}(10\bar{1}0)$ surfaces,³³ we find stable Mg-incorporated surfaces whose formation energies are lower than those for bare surfaces over the entire μ_{In} range.

Indeed, the structural features of top In and N atoms in these Mg-incorporated reconstructions are similar to those on InN(0001) and InN(000 $\bar{1}$) surfaces, respectively: All In adatoms at the top layer of the ideal surface are substituted by Mg atoms (the fraction of substitutional Mg at the topmost In site is 1) and topmost N atoms are attached to In adatoms forming an In adlayer with In-In bonds as shown in Figs. 4(b) and 4(d) (In_{adlayer}+2Mg_{In}, hereafter). The stabilization of these structures results from the formation of covalent In-In and In-N bonds.³⁴ Since the energy gain for Mg-incorporation in InN(11 $\bar{2}$ 0) surface (0.16-0.60 eV per Mg atom) is the largest over a wide μ_{In} range, it is expected that the (11 $\bar{2}$ 0) plane is most preferred for Mg-incorporation.

The reduction of surface carrier concentrations and the compensation of Mg acceptors on nonpolar planes can also be deduced from the DOS in Mg-incorporated InN(10 $\bar{1}$ 0) and (11 $\bar{2}$ 0) surfaces. Figure 5 illustrates the DOS of In_{adlayer}+2Mg_{In}, along with those of stable bare surfaces such as In_{bilayer} and In_{adlayer}. Obviously, the electronic states around the Fermi energy in bare surfaces (dashed line in Fig. 5) are reduced in In_{adlayer}+2Mg_{In} (solid line in Fig. 5), suggesting the reduction of electron concentration by Mg doping. Inspections of wave-functions clarify that the reduction of electronic states comes from the electron transfer from the In adlayer to Mg forming the bonding states between Mg and N atoms, and the formation of covalent In-In bonds along the [11 $\bar{2}$ 0] and [0001] directions for (10 $\bar{1}$ 0) and (11 $\bar{2}$ 0), respectively. As a result, In_{adlayer}+2Mg_{In} is stabilized and exhibits a semiconducting nature. Besides, we find that the local DOS for N atoms near the surface for In_{adlayer}+2Mg_{In} (dotted lines in Fig. 5) are occupied by electrons. Similar to the case of Mg-incorporated polar surfaces, Mg acceptors located at the nonpolar surfaces are expected to be compensated by electrons from the surfaces.

In summary, we have investigated the structures and electronic states of Mg-incorporated InN surfaces for various orientations. Our results provide immediate access to the atomic structure of Mg-incorporated surfaces under realistic growth conditions. For nonpolar orientations, we have proposed several Mg-incorporated reconstructions exhibiting a semiconducting nature.

Work at Mie University was supported in part by JSPS under Contract No. 21560032. Work at Northwestern University was supported by the NSF through its MRSEC program at Northwestern University (DMR 0520513). Computations were performed at RCCS (National

- ¹ J. Wu, W. Walukiewicz, K.M. Yu, J.W. Ager III, E.E. Haller, H. Lu, W.J. Schaff, Y. Saito, and Y. Nanishi, *Appl. Phys. Lett.* **80**, 3967 (2002).
- ² Y. Saito, H. Harima, E. Kurimoto, T. Yamaguchi, N. Teraguchi, A. Suzuki, T. Araki, and Y. Nanishi, *phys. stat. sol.(b)* **234**, 796 (2002).
- ³ R.E. Jones, K.M. Yu, S.X. Li, W. Walukiewicz, J.W. Ager, E.E. Haller, H. Lu, and W.J. Schaff, *Phys. Rev. Lett.* **96**, 125505 (2006).
- ⁴ P.A. Anderson, C.H. Swartz, D. Carder, R.J. Reeves, S.M. Durbina, S. Chandril and T.H. Myers, *Appl. Phys. Lett.* **89**, 184104 (2006).
- ⁵ V. Cimalla, M. Niebelschutz, G. Ecke, V. Lebedev, O. Ambacher, M. Himmerlich, S. Krischok, J. A. Schaefer, H. Lu, and W. J. Schaff, *phys. stat. sol. (a)* **203**, 59 (2006)
- ⁶ X. Wang, S.-B. Che, Y. Ishitani, and A. Yoshikawa, *Appl. Phys. Lett.* **90**, 201913 (2007).
- ⁷ J.-H. Song, T. Akiyama, and A.J. Freeman, *Phys. Rev. Lett.* **101**, 186801 (2008).
- ⁸ P. Waltereit, O. Brandt, A. Trampert, H. T. Grahn, J. Menniger, M. Ramsteiner, M. Reiche, and K. H. Ploog, *Nature* **406**, 865 (2000).
- ⁹ M. Mclaurin, B. Haskell, S. Nakamura, J.S. Speck, *J. Appl. Phys.* **96**, 327 (2004).
- ¹⁰ T. Takeuchi, S. Sota, M. Katsuragawa, M. Komori, H. Takeuchi, H. Amano, and I. Akasaki, *Jpn. J. Appl. Phys.* **36**, L382 (1997).
- ¹¹ P.D.C. King, T.D. Veal, C.F. McConville, F. Fuchs, J. Furthmuller, F. Bechstedt, P. Schley, R. Goldhahn, J. Schormann, D.J. As, and K. Lischk, D. Muto, H. Naoi, Y. Nanishi, H. Lu and W.J. Schaff, *Appl. Phys. Lett.* **91**, 092101 (2007).
- ¹² C.-L. Wu, H.-M Lee, C.-T. Kuo, C.-H Chen, and S. Gwo, *Phys. Rev. Lett.* **101**, 106803 (2008).
- ¹³ D. Segev and C.G. Van de Walle, *Surf. Sci.* **601**, L15 (2007).
- ¹⁴ C.G. Van de Walle and D. Segev, *J. Appl. Phys.* **101**, 81704 (2007).
- ¹⁵ J.P. Perdew, K. Burke, and M. Ernzerhof, *Phys. Rev. Lett.* **77**, 3865 (1996).
- ¹⁶ N. Troullier and J.L. Martins, *Phys. Rev. B* **43**, 1993 (1991).
- ¹⁷ D. Vanderbilt, *Phys. Rev. B* **41**, 7892 (1990).
- ¹⁸ S.G. Louie, S. Froyen, and M.L. Cohen, *Phys. Rev. B* **26**, 1738 (1982).
- ¹⁹ Our calculations using $4d$ states as valence electrons have found that effects of the pseudopo-

tential modification on the structural and electronic properties for the In pseudopotential with partial core corrections (PCC) are identical to those for the In pseudopotential including $4d$ electrons as the valence band. The overall band structures near the Fermi level using PCC agree with those using $4d$ valence electrons within 0.1-0.2 eV, and the accuracy of the total-energy difference between different structures is estimated to be within ~ 0.1 eV. Furthermore, our results agree well with the previous calculations by D. Segev, A. Janotti, and C.G. Van de Walle, Phys. Rev. B **75**, 035201 (2007) and Ref. 14.

- ²⁰ J. Yamauchi, M. Tsukada, S. Watanabe, and O. Sugino, Phys. Rev. B **54**, 5586 (1996).
- ²¹ C.K. Gan and D.J. Srolovitz, Phys. Rev. B **74**, 115319 (2006).
- ²² *CRC Handbook of Chemistry and Physics*, ed. David R. Lide (CRC Press, Florida, 1999), 80th ed.
- ²³ Y. Kangawa, T. Ito, A. Taguchi, K. Shiraishi, and T. Ohachi, Surf. Sci. **493**, 178 (2001).
- ²⁴ C.G. Van de Walle and J. Neugebauer Phys. Rev. Lett. **88**, 066103 (2002).
- ²⁵ We have examined in total more than 60 different structures. The figures of formation energy include only those reconstructions that are found to be energetically favorable in some part of the phase space spanned by the chemical potentials.
- ²⁶ T.D. Veal, P.D.C. King, P.H. Jefferson, L.F. J. Piper, C.F. McConville, H. Lu and W. J. Schaff, P.A. Anderson, S.M. Durbin, D. Muto, H. Naoi, and Y. Nanishi, Phys. Rev. B **76**, 075313 (2007).
- ²⁷ J.E. Northrup, Appl. Phys. Lett. **86**, 122108 (2005).
- ²⁸ Q. Sun, A. Selloni, T.H. Myers, and W.A. Doolittle, Phys. Rev. B **73**, 155337 (2006).
- ²⁹ M. D. Pashley, Phys. Rev. B **40**, 10481 (1989).
- ³⁰ T. Miyajima, S. Uemura, Y. Kudo, Y. Kitajima, A. Yamamoto, D. Muto, and Y. Nanishi, phys. stat. sol.(c) **5**, 1665 (2008).
- ³¹ T. Ito and K. Shiraishi, Jpn. J. Appl. Phys. **35**, L949 (1996).
- ³² The Mg-doping on InN(000 $\bar{1}$) plane has been performed under N-rich condition. See, D. Muto, H. Naoi, S. Takado, H. Na, T. Araki, and Y. Nanishi, Mater. Res. Soc. Symp. Proc. **955**, I08-01 (2007).
- ³³ J.E. Northrup, Phys. Rev. B **77**, 045313 (2008).
- ³⁴ Compared to the ideal surface, the energy gain of Mg-incorporation is ~ 0.5 eV per Mg atom. This comes from the energies of In-N bond (2.0 eV) and covalent In-In bonds (1.5 eV), the

energy difference between In-N and Mg-N bonds (~ -0.1 eV), and the chemical potential shift due to the gas-phase Mg (-2.5 eV).

Figures

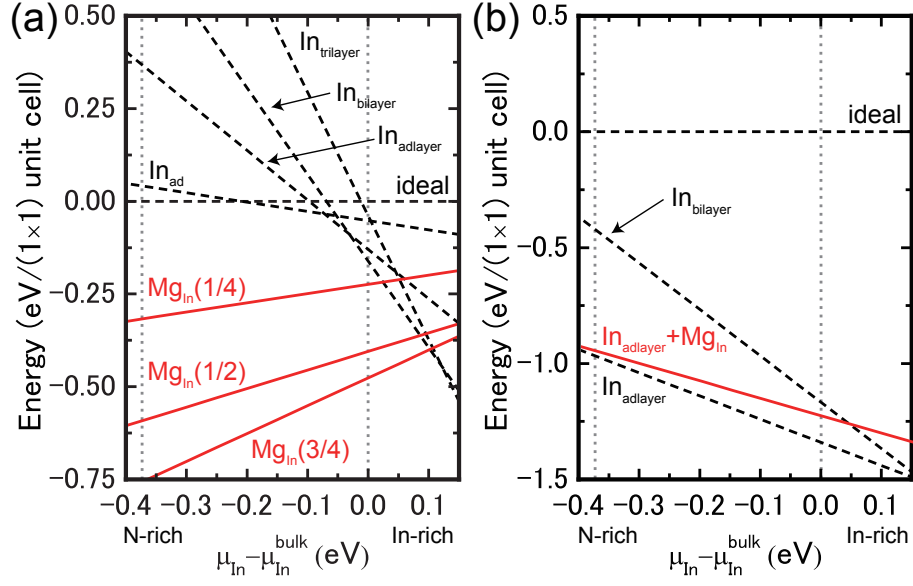


FIG. 1: (Color online) Calculated formation energies of Mg-incorporated (a) InN(0001) and (b) InN(000 $\bar{1}$) surfaces (solid lines) using Eq. (1) as a function of μ_{In} , along with those for bare surfaces (dashed lines). The value of μ_{Mg} are $E_{\text{Mg}} - 2.5$ and $E_{\text{Mg}} - 2.7$ eV, which correspond to Mg-rich conditions ($p = 1.0 \times 10^{-7}$ Torr) at $T = 725$ and 825 K for InN(0001) and InN(000 $\bar{1}$) surfaces, respectively.

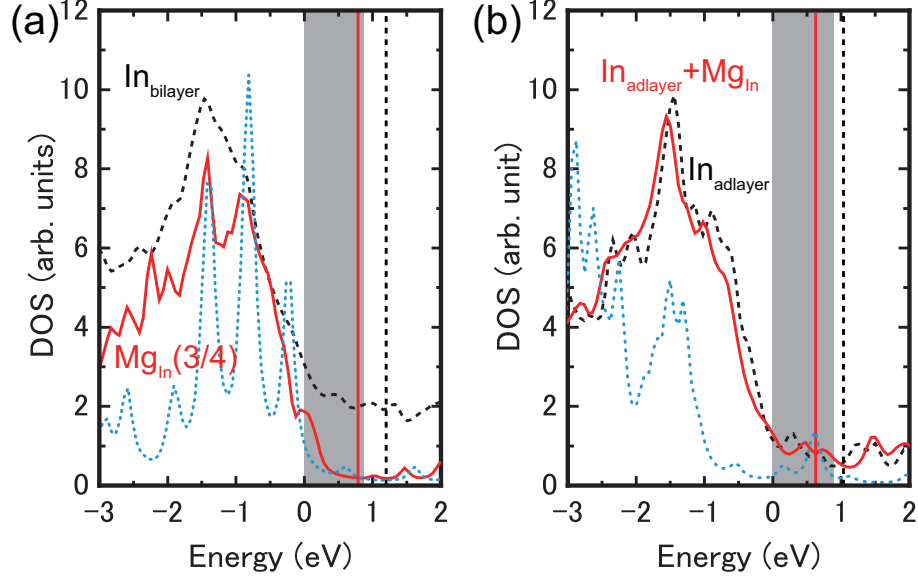


FIG. 2: (Color online) Density of states (DOS) for (a) laterally contracted In-bilayer structure ($\text{In}_{\text{bilayer}}$) and the 2×2 surface with three substitutional Mg atoms ($\text{Mg}_{\text{In}}(3/4)$) by Mg-incorporation on InN(0001) surface, and for (b) In-adlayer reconstruction ($\text{In}_{\text{adlayer}}$) and In-adlayer structure with substitutional Mg ($\text{In}_{\text{adlayer}} + \text{Mg}_{\text{In}}$) on InN(0001) surface. The local DOS of N atom near the surface for $\text{Mg}_{\text{In}}(3/4)$ and $\text{In}_{\text{adlayer}} + \text{Mg}_{\text{In}}$ is also shown by blue (dotted) lines. The energy gap obtained from bulk VBM and CBM in the band structure of Mg-incorporated InN surfaces is shown by shaded region. The zero of energy is set at the VBM. The vertical solid and dashed lines denote the Fermi energies of Mg-incorporated and bare surfaces, respectively.

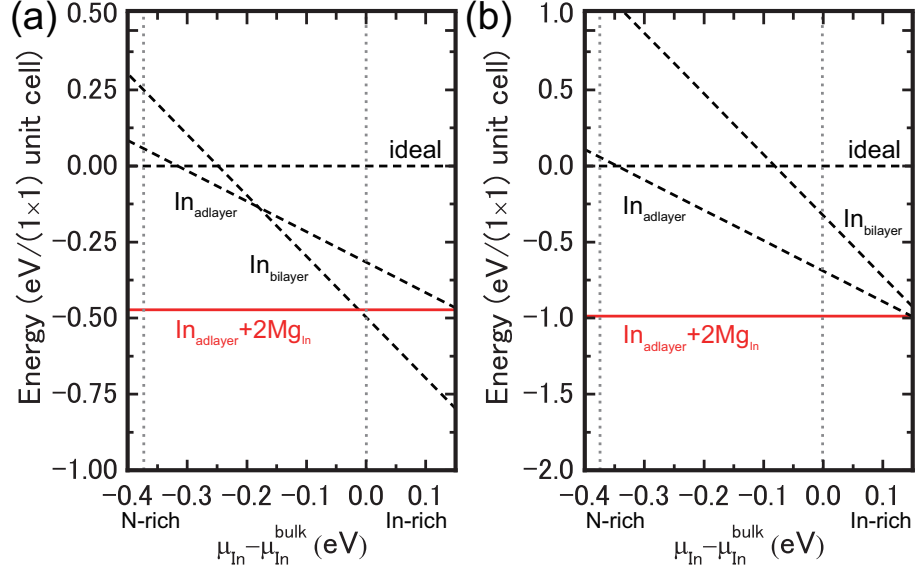


FIG. 3: (Color online) Calculated formation energies of Mg-incorporated (a) $\text{InN}(10\bar{1}0)$ and (b) $\text{InN}(11\bar{2}0)$ surfaces (solid lines) using Eq. (1) as a function of μ_{In} , along with those for bare surfaces (dashed lines). The value of μ_{Mg} is $E_{\text{Mg}} - 2.5$ eV, which corresponds to Mg-rich conditions ($p = 1.0 \times 10^{-7}$ Torr) at $T = 725$ K.

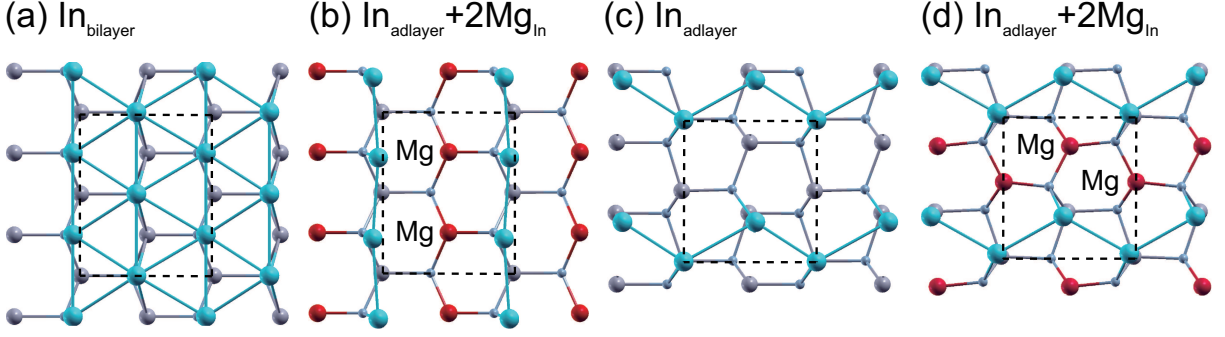


FIG. 4: (Color online) Schematic top views of (a) $\text{InN}(10\bar{1}0)$ with In bilayer ($\text{In}_{\text{bilayer}}$), (b) Mg-incorporated $\text{InN}(10\bar{1}0)$ with In adlayer ($\text{In}_{\text{adlayer}} + 2\text{Mg}_{\text{In}}$), (c) $\text{InN}(11\bar{2}0)$ with In adlayer ($\text{In}_{\text{adlayer}}$), and (d) Mg-incorporated $\text{InN}(11\bar{2}0)$ with In adlayer. Large and small gray circles represent In and N atoms, respectively. Red (black) circles denote Mg atoms and blue (light-gray) circles top-layer In atoms. The unit cell used in this study is shown by dashed rectangle.

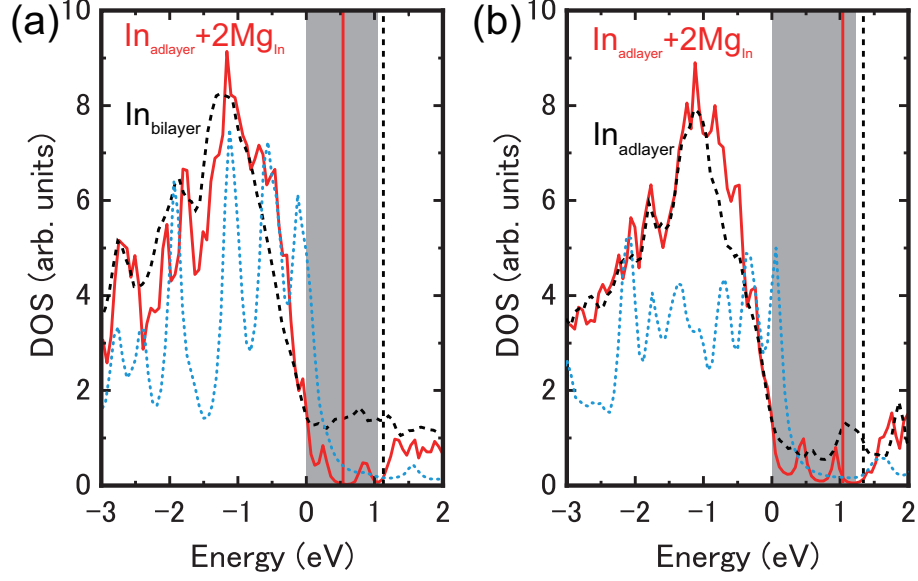


FIG. 5: (Color online) Density of states (DOS) for (a) laterally contracted In-bilayer structure ($\text{In}_{\text{bilayer}}$) and In-monolayer surface with two substitutional Mg atoms ($\text{In}_{\text{adlayer}}+2\text{Mg}_{\text{In}}$) by Mg-incorporation on $\text{InN}(10\bar{1}0)$ surfaces, and for (b) $\text{InN}(11\bar{2}0)$ surface with In adlayer ($\text{In}_{\text{adlayer}}$) and In-adlayer surface with two substitutional Mg atoms ($\text{In}_{\text{adlayer}}+2\text{Mg}_{\text{In}}$). Note that the gap energies obtained by the calculations of $\text{InN}(10\bar{1}0)$ and $(11\bar{2}0)$ surfaces are larger than that in the bulk case by 0.4 and 0.5 eV, respectively. The same notation as in Fig.2